IAC-08-C1.2.10

COMPARATIVE STUDY ON THE APPLICATION OF EVOLUTIONARY OPTIMIZATION TECHNIQUES TO ORBIT TRANSFER MANEUVERS

Edmondo A. Minisci
Department of Aerospace Engineering, University of Glasgow, Scotland
e-mail: *eminisci@eng.gla.ac.uk*

Giulio Avanzini
Department of Aerospace Engineering, Politecnico di Torino, Italy
e–mail: *giulio.avanzini@polito.it*

Abstract

Orbit transfer maneuvers are here considered as benchmark cases for comparing performance of different optimization techniques in the framework of direct methods. Two different classes of evolutionary algorithms, a conventional genetic algorithm and an estimation of distribution method, are compared in terms of performance indices statistically evaluated over a prescribed number of runs. At the same time, two different types of problem representations are considered, a first one based on orbit propagation and a second one based on the solution of Lambert's problem for direct transfers. In this way it is possible to highlight how problem representation affects the capabilities of the considered numerical approaches.

1. Introduction

In this paper the performance of different optimization techniques are analyzed and compared in the framework of the determination of minimum fuel – minimum time orbit maneuvers. In particular, two different evolutionary methods, namely a conventional Multi Objective Genetic Algorithm (MOGA) [1] and the Multi-Objective Parzen-Based Estimation of Distribution Algorithm (MOPED) [2], are combined with a standard orbit propagation code and a new solution method for Lambert problem [3], resulting in a total of four possible optimization approaches.

Optimization of orbit maneuvers has been investigated for a long time, and many different approaches have been proposed in the scientific literature. The long standing interest for this class of problems is apparent, when one considers the importance of achieving a prescribed orbit within a given time frame while minimizing the amount of fuel used. Any saving on fuel required for a given (set of) maneuver(s) results into either a longer operational life (more maneuvers can be performed given the amount of fuel available at the beginning of the mission), a higher available payload for the same launch weight (where a higher probe weight at the end of an interplanetary travel means more scientific instruments on board), a smaller total launch weight (which immediately results into a reduction of launcher weight and cost), or any combination of the above possibilities.

For this reason, reliable optimization procedures are of paramount importance during all phases of space mission analysis and design, from preliminary steps, where the mission scenario can be simplified in order to achieve a quick idea of viable solutions, to the design of the sequence of operations, where each mission step is addressed in order to estimate as carefully as possible operational requirements.

From the mathematical standpoint, the minimization problem is often made more complex by engineering constraints. In simple cases, the total mission time and/or the transfer time must lie within prescribed limits or a given target orbit must be reached within tight accuracies. In more complex scenarios a certain sequence of events must take place in either a prescribed place or at a prescribed time, e.g. because of requirements on communications with the ground station. The resulting optimization problem is often a multi–modal one, where local minima seriously challenge the convergence capability of optimization algorithms onto a global optimal solution.

Several approaches were proposed in the past, the major distinction being between direct and indirect methods, where the latter class of methods, based on the solution of optimization problems in terms of Pontryagin principle (see, *e.g.*, [4–6], and references therein), will not be considered in the sequel. Direct methods are based on the expression of the objective function and operational constraints as a function of a finite set of mission design variables. Minimization of

the function is pursued starting from one or more initial guesses until some convergence criterion is satisfied.

Direct methods based on steepest descent approaches (such as gradient based methods or sequential–quadratic programming) are fast and sufficiently reliable, from the numerical standpoint, when the optimization problem is well–behaved. Unfortunately, given an initial guess, the algorithm converges onto a local minimum lying inside the same convex basin of attraction, so that extensive computation is necessary to span the whole search space when a global minimum is searched. Constraints can be enforced by either a penalty method or by a Lagrange multipliers approach [7], but sometimes even finding a single feasible solution may not be a trivial task. The optimization problem can easily become ill–conditioned because of the presence of tight or competing constraints that prevents the algorithm from converging.

For all these reasons evolutionary algorithms (EAs) offer an interesting alternative [8], where rather than a purely random search or a computationally expensive systematic search on regular grids, the evolution of a population of candidate solutions is driven towards a global optimum by the fitness of its individuals. The computational effort is still considerable, but it is usually possible to span selected portions of the search space while leaving out of the analysis those regions where an optimal solution is less likely to be found. As a further advantage it is easier to tackle multi–objective problems by means of the dominance criterion [1]. If a steepest descent method was employed, this situation would require the solution of several minimization processes of a weighted combination of the considered merit functions for different values of the weights.

Evolutionary algorithms include a very wide range of numerical procedures, that range from genetic algorithms (GAs) [9] to evolutionary strategies (ESs) [10] and differential evolution (DE) [11]. They are a powerful global optimization method, and, although convergence to a global optimum is only guaranteed in a weak probabilistic sense, they are well suited for a wide range of both combinatorial and continuous problems.

Surprisingly enough, a systematic comparison of different optimization techniques has been seldom considered in the literature, in spite of the fact that different approaches may achieve different performance depending on the considered problem. Although some works proposed a comparison between pairs of algorithms over some specific problem, [12,13], a first attempt to identify those global optimization algorithms that outperform all others over different classes of orbit transfer problems (namely two–impulse transfers, low–thrust transfer and low–energy transfers in the framework of the restricted three–body problem) was developed by Di Lizia *et al.* [14], demonstrating that differential evolution methods perform particularly well on most of the problems, compared to other algorithms. More recently, Vasile *et al.* [15] proposed some performance metrics for comparing global optimization methods, discussing the actual significance of the considered performance indexes and proposing some criteria to evaluate the actual usefulness of each algorithm. They addressed specifically black–box problems in space trajectory design, focusing their attention on stochastic based approaches.

As a matter of fact, there are different (and often competing) metrics that must be considered when comparing the performance of optimization algorithms, especially when dealing with evolutionary methods (number of function evaluations, accuracy of the solution, capability of converging onto the global optimum, repeatability of the solution, and so on), so that it is often not trivial to identify the "best" algorithm in every respect. Moreover, together with the type of orbit transfer and the class of optimization method employed, the representation of the orbital problem may play a role in the capabilities demonstrated by an optimization algorithm, because of the characteristics of the resulting search space and its functional relation with the objective function(s).

The scope of this paper is twofold: together with a contribution to the discussion on suitable metrics for the comparison of optimization approaches in the framework of orbit maneuvers and how to combine them into a comparison criterion, the effects of problem representation on the obtained results is also considered, in order to analyze if and how this latter aspect affects the performance of optimization algorithms. Rather than spanning all the possible situations and types of orbit transfers, only direct two– and three–impulse transfers will be considered as test benchmarks for the considered classes of EAs: a standard GA, the nowadays classic Non–Dominated Sorting Genetic Algorithm–II (NSGA–II) [16], where the evolution is driven by stochastic operators that mimic the natural process of selection, mating and mutation, and the MOPED algorithm, where a probabilistic approach is employed by randomly generating a population from the reconstruction of a probability density function obtained from the evaluation of the fitness of individuals from the previous generation. For all the considered applications, the optimization is achieved in the framework of multi–objective problems, where Pareto fronts in the minimum time – minimum fuel plane are traced.

The metrics used for evaluating algorithm performance are based on the capabilities demonstrated by the four considered optimization approaches over several runs for each one of the considered cases, as already pointed out in [15], where single–objective optimizations were considered. As a matter of fact, repeatability

of the results is one of the most important aspects, when dealing with stochastic methods. This means that the computation effort for a reliable evaluation can become overwhelming, when multi–objective problems are considered, the solution of which is not a single optimal solution but a whole population spread along the Pareto front. Since it is not possible to perform an infinite number of runs for each case, it would be important to estimate the error on the indexes computed for a limited number of tests, which can be very low, depending on the available computational resources. In the framework of this preliminary analysis, only 20 runs for each case were performed, and results are analyzed on the basis of the confidence level. A more detailed statistical analysis of the actual properties of the index distributions will be considered as the next step of this research. For the same reason the analysis was limited to relatively simple orbit transfer cases.

The two optimization algorithms are briefly presented in the next Section of the paper. More details can be found in [16], [2] and [12]. In Section 3, after presenting problem geometry, objectives and constraints, two different orbit transfer parameterizations are considered. The first one is based on the use of velocity increment components as optimization variables, where the f-g method based on Lagrangian coefficients [17] is employed for propagating the orbits along coasting arcs between thrust impulses, thus solving a shooting problem. In the second case the transfer orbit is determined by means of the solution of the Lambert problem [17,3], where the considered initial and final positions represent the optimization variables. Then, a discussion on possible metrics for evaluating algorithm performance is reported in Section 4.

In Section 5 a first set of results deals with a very simple problem, that is, the coplanar transfer between circular orbits, the minimum–fuel solution of which is the well–known Hohmann transfer. This is done in order to compare the obtained results with those presented in the available literature [12,18–20]. A second simple example, namely the direct transfer between coplanar generic elliptical orbits, allows for a visualization of the comparison because of the small dimension of the search space. In this way it is possible to refine the definition of the metrics for the evaluation of the performance of different optimization algorithm with respect to analytically determined results. Two more complex problems are finally considered, with wider search spaces: a three impulse transfer [19,20] and the simultaneous transfer of two spacecraft from the same Low Earth Orbit (LEO) to different positions on the geostationary orbit (GEO) [12]. A Section of Conclusions ends the paper.

2. Evolutionary Optimization methods

For this work two multi-objective optimization algorithm are used. The first is a standard Genetic Algorithm (GA), the NonDominated Sorting Genetic Algorithm-II (NSGA-II), which still represents one of the best multi-objective GA (MOGA) in the literature. The second one is an Evolutionary Algorithm (EA) which belongs to the sub-class of Estimation of Distribution Algorithms (EDAs). A brief description of both algorithms is here presented, pointing out similarities and main differences, in order to allow the reader to better understand the analysis of the reported results.

2.1 Non–Dominated Sorting Genetic Algorithm–II (NSGA-II)

In the NSGA-II the dominance depth is used to classify the population. A crowding parameter is also determined in order to rank the individuals inside each class of dominance. For each element of a class, the crowding parameter is obtained as the sum of the difference of the cost functions of the nearest elements in the cost function space, divided by the range spanned by the population with respect to each objective function. Inside each class, the individuals with the higher value of the crowding parameter obtain a better rank than those with a lower one, forcing to explore the Pareto front.

The unconstrained version of the algorithm can be briefly described as follows. Initially, a random parent population $\mathcal{P}_0$ is created. The population is sorted by means of the non-domination criterion, whereas each individual is assigned a fitness parameter equal to its non–domination level. A fitness value equal to 1 (best cases) is assigned to the non–dominated individuals, that form the first layer. Those individuals dominated only by members of the first layer form the second one and are assigned a fitness value of 2, and so on. In general, for dominated individuals, the fitness is given by the number of dominating layers plus 1 and minimization of fitness index is pursued by the algorithm.

Binary tournament selection, recombination, and mutation operators [16] are used to create a child population $\mathcal{Q}_0$ of size N_{ind} for the initial generation. Given a parent and a child generation, indicated by the subscript $t \geq 0$, the procedure is based upon generation of a combined population $\mathcal{R}_t = \mathcal{P}_t \oplus \mathcal{Q}_t$ of size $2N_{ind}$. Then, $\mathcal{R}_t$ is sorted according to the non–domination criterion. The new parent population $\mathcal{P}_{t+1}$ of size N_{ind} is formed by first sorting the members of the last front according to the crowding comparison operator and then picking up the first N_{ind} individuals that form $\mathcal{P}_{t+1}$.

The new parent population can now be used for selection, crossover and mutation to create a new child population $\mathcal{Q}_{t+1}$ of size N_{ind} and iterate the process.

In this work the real-coded, constrained version (simulated binary crossover, SBX, and polynomial mutation) has been used. Constraints were handled according to the constraint-domination principle [16], which discriminates between unfeasible and feasible solution during the non–dominated sorting procedure. The definition of constrained–domination is: a solution i is said to constrained–dominate a solution j, if (a) solution i is feasible and solution j is unfeasible; or (b) solution i and j are both unfeasible, but solution i is closer to the constraint boundary; or (c) if both solutions are feasible but i dominates j with respect to the objectives functions.

The parameters to be set are: size of the population, N_{ind}, crossover probability, p_c, mutation probability, p_m, and distribution indexes for crossover and mutation, η_c and η_m, respectively.

2.2 Multi-Objective Parzen-Based Estimation of Distribution Algorithm (MOPED)

The MOPED algorithm is a multi-objective optimization algorithm for continuous problems that uses the Parzen method to build a probabilistic representation of Pareto solutions, with multivariate dependencies among variables. The Parzen method [4] pursues a non-parametric approach to kernel density estimation and it gives rise to an estimator that converges everywhere to the true Probability Density Function (PDF) in the mean square sense. Should the true PDF be uniformly continuous, the Parzen estimator can also be made uniformly consistent. In short, the method allocates exactly N_{ind} identical kernels, each one centered on a different element of the sample.

Similarly to what was done in [21] for multi-objective Bayesian Optimization Algorithm (moBOA), some techniques of NSGA-II are used to classify promising solutions in the objective space, while new individuals are obtained by sampling from the Parzen model. NSGA-II was identified as a promising base for the algorithm mainly because of its intuitive simplicity coupled with brilliant results on many problems. The major differences between MOPED and NSGA-II, due to the classification and search techniques, are recalled in the sequel.

2.2.1 Classification and Fitness evaluation

The individuals of the population are classified in a way that favors the most isolated individuals in the objective function space, in the first sub-class (highest dominance) of the first class (best suited with respect to problem constraints).

If the problem is characterized by m constraints $c_i(\boldsymbol{x})$, $i = 1, 2, ..., m$, such that $c_j(\boldsymbol{x}) = 0$ indicates that the j–th constraint is satisfied, the first step in the evaluation of the fitness parameter is the determination of the degree of compatibility of each individual with the constraints. The compatibility, indicated by the symbol cp, is measured as the weighted sum of unsatisfied constraint. Once the value of cp is evaluated for all the individuals, the population is distributed over a predetermined number of classes, $1 + N_{cl}$. The N_{best} individuals that satisfy all the constraints, such that $cp = 0$, are in the first class. The remainder of the population is divided in the other groups, each one containing an approximately equal number of individuals, given by $\text{round}(N_{ind} - N_{best})/N_{cl}$.

The second class is formed by those individuals with the lower values of the constraint parameter and the last one by those with the highest values. For each class, individuals are ranked in terms of dominance criterion and crowding distance in the objective function space, using the NSGA-II techniques. After ranking all the individuals of the population, from the best to the worst one, depending on their belonging to a given class and dominance level and the value of their crowding parameter, a fitness value f linearly varying from $2 - \alpha$ (best individual of the entire population) to α (worst individual), with $\alpha \in [0; 1)$, is assigned to each individual. This fitness value determines the weighting of the kernel for sampling the individuals of the next generation. As an example, for $\alpha = 0$, the best solution ($f = 2$) provides a kernel with twice as much possibilities of generating new individuals for the next generation than the central one, placed at half of the classification (for a corresponding value of $f = 1$), while the kernel for the worst one ($f = 0$) is prevented from generating new individuals. Higher values of α are usually employed for allowing sampling of regions of the search space far from the current best solutions.

2.2.2 Building the model and sampling

As briefly outlined in the previous section, a probabilistic model of the promising search space portion is built on the basis of the information given by N_{ind} individuals of the current population, by means of the Parzen method. On the basis of this model, τN_{ind} new individuals, with $\tau \geq 1$ are sampled. The variance associated to each kernel depends on (i) the distribution of the individuals in the search space and (ii) on the fitness value associated to the pertinent individual, so as to favor sampling in the neighborhood of the most promising solutions. For generic processes it can be useful to alternatively adopt different kernels from a generation to the other, in order to improve the exploration of the search space.

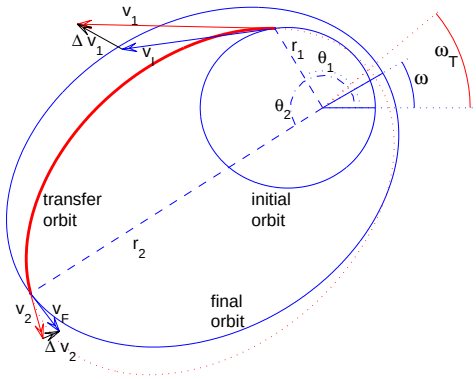

Figure 1: Geometry of the orbit transfer

The parameters to be set for the MOPED algorithm are: size of the population, N_{ind}, number of constraint classes, N_{cl}, the fitness coefficient, α, the sampling proportion, τ.

3. Problem Statement

3.1 Geometry, Objectives and Constraints

The geometry of a generic two–impulse coplanar orbit transfer is depicted in Fig. 1. Both the initial and the target orbits are defined by means of their orbital elements, indicated by the subscript I and F, respectively. Problem geometry is defined by 6 quantities only, namely semi–major axis, a_I and a_F, eccentricity, e_I and e_F, angle between the periapsis, $\Delta\omega$, and initial spacecraft position on the initial orbit, θ_{σ_0}. Assuming the periapsis of the initial orbit as reference for angles, the argument of the periapsis for the initial and target orbits are $\omega_I = 0$ an $\omega_F = \Delta\omega$, respectively.

The transfer is accomplished by means of two impulses, $\Delta\vec{\boldsymbol{v}}_1$ and $\Delta\vec{\boldsymbol{v}}_2$, identified by their magnitude $\Delta v = ||\Delta\vec{\boldsymbol{v}}||$ and angle with respect to the tangential direction, ϕ. The first impulse at time $t_1 = t_W$ (where t_W indicates the waiting time on the initial orbit) injects the spacecraft on the transfer orbit (thick line in Fig. 1); the second one at time $t_2 = t_F = t_1 + t_T$ (where t_T is the transfer time) injects the spacecraft on the target orbit and completes the prescribed maneuver. The parameters of the transfer orbit will be identified by the subscript T.

If the initial orbit is circular, its periapsis is not defined and the periapsis of the target orbit is assumed as reference for the anomalies. If both orbits are circular, as for the Hohman transfer case, the problem is symmetric and the spacecraft position at injection time has no influence on the transfer, so that $t_1 = 0$ and $\theta_{\sigma_0} = 0$ are assumed without loss of generality.

In all the considered cases, one of the objective functions is the total velocity increment, namely

$$\Delta v_{tot} \quad = \quad ||\Delta\vec{\boldsymbol{v}}_1|| + ||\Delta\vec{\boldsymbol{v}}_2||$$

The total transfer time, given by the sum of waiting and transfer times, t_F, is included in the analysis as the second merit function, for multi–objective optimization. If a rendez–vous problem is dealt with, a further problem parameter is the target position at the initial time, θ_{τ_0}. In such a case a constraint on the final spacecraft position is represented by the condition $\theta_{\sigma_2} = \theta_{\tau_2}$, where the subscripts σ and τ indicate spacecraft and target, respectively.

Other constraints are included in the analysis. In particular, only arcs of elliptic orbits will be considered as admissible transfer trajectories, so that a first constraint is

$$e_T < 1$$

When considering planet centered orbits, the transfer orbit must remain higher than a prescribed minimum over the surface. Such a condition is enforced by means of the inequality

$$r_{T,min} \geq k r_{P_I},$$

where $r_{T,min}$ is the minimum radius along the transfer orbit arc, while $r_{P_I} = a_I(1 - e_I)$ is the initial orbit periapsis and $k \leq 1$ is a prescribed coefficient. Note that if the transfer orbit periapsis lies outside of the considered transfer arc, it is $r_{T,min} = r_1 \geq r_{P_I}$, and the constraint is not active.

3.2 Definition of benchmark cases

As stated in the Introduction, this preliminary analysis is focused more on the methodological aspects of the problem of comparing different optimization approaches, including how the orbit transfer is represented in the optimization process. For this reason, only relatively simple cases (two–impulse transfers between circular and elliptical orbits, three–impulse transfer with rendez–vous on the target orbit and a simultaneous two–impulse transfer for two formation–flying satellites) are considered as test benchmarks for the considered approaches. All the relevant data relative to these cases are summarized in Tab. 1. These cases are sufficient for outlining the major findings of this preliminary study. More complex scenarios will be the object of forthcoming research.

3.2.1 Case 1: Direct transfer between circular orbits

Case 1 deals with minimum–fuel/minimum–time direct transfer between circular orbits. Although the optimal

Table 1: Orbits for benchmark cases

Case	No. of satellites	Planet	μ		a_I		e_I	a_F		e_F
1	1	Mars	4.2828 10^4	km^3s^{-2}	8 000	km	0	15 000	km	0
2	1	Earth	3.9860 10^5	km^3s^{-2}	6 721	km	0	26 610	km	0.667
3	1	Earth	3.9860 10^5	km^3s^{-2}	7 000	km	0	42 000	km	0
4	2	Earth	3.9860 10^5	km^3s^{-2}	7 000	km	0	42 000	km	0

solution can be derived analytically (the well–known Hohmann transfer, for the minimum–fuel problem [17]), this case was often used in the past as a preliminarily assessment of the capabilities of EAs in the framework of orbit maneuver optimization [18–20]. In particular, [18] and [19] represent two of the first examples of applications of GAs to orbit maneuver problems, while [12] offers maybe the first attempt of comparing different evolutionary approaches on the same problem, although in a relatively qualitative way.

The case considered, taken from [20], is the transfer between two circular Mars orbits of different radii. As a difference with respect to the cited applications of GAs, both fuel consumption and trasfer time are assumed as objective functions to be minimized so that the Hohmann transfer represents one of the extremes of the Pareto front in the Δv_{tot}–t_T plane.

Together with the constraint on the eccentricity of the transfer orbit, $e < 1$, the minimum distance constraint is also enforced with $k = 1$. The geometry of the problem is defined by the ratio of the radii, r_F/r_I, and the waiting time has no influence on the transfer (including the optimal one), because of the radial symmetry of the problem.

3.2.2 Case 2: Direct transfer with rendez–vous

A slightly more complex case was considered by A. Reichert in her work [18], where transfers between generic elliptical orbits were also dealt with. Only if the ellipses are aligned a Hohmann–like optimal transfer is easily determined. In the general case, the lines of the apsides of the two orbits form a certain angle, $\Delta\omega$, and the variation of Δv_{tot} as a function of the extremes of the transfer arc is more complex.

The geometry of the problem is described by a higher number of parameters, namely the ratio of the semi–major axes, a_F/a_I, the eccentricities, e_I and e_F, and the angle $\Delta\omega$. The solution depends on the initial spacecraft positions, θ_σ at time $t = 0$, even when the initial orbit is circular (e.g. a circular LEO), so that $e_I = 0$ and $\Delta\omega$ is no longer defined.

In this paper, a further constraint is added on the final position, that is, the spacecraft must reach a target on the final orbit (rendez–vous problem). In this scenario the solution depends also on the initial position of the target, θ_τ at time $t = 0$. A further constraint is introduced on the final position, $\theta_\sigma = \theta_\tau$ at time $t = t_F \equiv t_2$.

The data used for Case 2 and reported in Tab. 1 are representative of a transfer from a circular LEO to a high eccentricity semisynchronous orbit. The transfer depends on two parameters only, namely t_W and t_T. Figure 2 represents a contour plot of Δv_{tot} as a function of these two parameters (white < 3 m/s, black > 15 m/s). The shaded areas represent unfeasible solutions where constraints on eccentricity and/or minimum radius are violated. The variation of Δv_{tot} in the t_W–t_T plane is characterized by several local minima. As a consequence, the Pareto front in the Δv_{tot}–t_T plane is expected to exhibit several arcs.

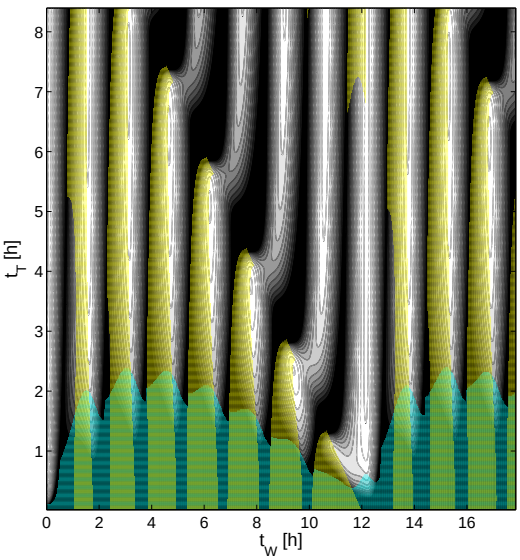

Figure 2: Δv for Case 2.

3.2.3 Case 3: Three–impulse transfer

The third case considered in this paper is a three–impulse transfer between circular orbits. Given the geometry of the initial and final orbits, a third impulse is allowed during the transfer, which is thus divided into two arcs. In such a case the solution space to be spanned becomes wider.

Similar cases were also analyzed in [19] and [20], although for different geometries and, apparently, with the only purpose of demonstrating the possibility of generalizing the optimization approach to a generic n–impulse transfer. In the present application a constraint on the final position is considered, so that the intermediate velocity increment can be used to correct the trajectory along the path and make the rendez–vous with the target somehow easier. Constraints on the eccentricity and minimum distance from the planet surface are enforced for both arcs, exactly as for the two–impulse transfer.

3.2.4 Case 4: Simultaneous transfer of 2 satellites

A final more complex application is considered, where two formation–flying satellites, indicated by the letters A and B are launched simultaneously from the same position on LEO towards two prescribed longitudes on GEO shifted by an angle $\Delta\lambda$ [12]. In this case the algorithm minimizes the total Δv required by the formation, $\Delta v_{FF} = \Delta v_{tot,A} + \Delta v_{tot,B}$, and the maneuver time t_{man}, that is, the time at which the last spacecraft achieves its prescribed position, $t_{man} = \max(t_{2,A}, t_{2,B})$.

As a matter of fact, two–impulse orbit transfers between circular orbits is considered with the constraint that the initial position is the same for both satellites. Also the constraints considered for Cases 2 and 3 apply in the same form as before to both spacecraft.

3.3 Representation of Orbit Transfers

In this paragraph the functional dependencies of merit functions and constraints with respect to the unknowns of the optimization problem will be expressed, in order to highlight the differences between the two considered representations of the orbit transfer problem for Keplerian motion: the first one, based on a standard orbit propagation algorithm (f-g method based on Lagrangian coefficients); the second based on the solution of the Lambert problem.

In this latter case the required Δv is obtained after the solution of the Lambert problem as a function of the orbit parameters of the orbit that contains the transfer arc, while in the first case magnitude and direction of the velocity increment are among the optimization variables, while the final position and transfer time are obtained from orbit propagation. As a consequence number of optimization variables (that is, the dimension of the search space) and the representation (or even the presence) of constraints may vary, when describing the transfer in different terms, thus affecting the performance of the optimization algorithm used.

3.3.1 Orbit propagation

When orbit propagation is used for determining the optimal two–impulse transfer, the optimization variables are magnitude and direction of the velocity increment of the two impulses, namely Δv_1 and ϕ_1 for the first impulse, and Δv_2 and ϕ_2 for the second one (where the angle ϕ_i is counted with respect to the local tangent to the orbit), together with the orbital anomalies θ_1 and $\theta_2 = \theta_1 + \Delta\theta$ of the corresponding positions. The vector of optimization variables is thus given by

$$\boldsymbol{x} = (\theta_1, \Delta v_1, \phi_1, \Delta\theta, \Delta v_2, \phi_2)^T \in \mathbb{R}^6$$

A total of 5 constraints is enforced: 3 equality constraints on semi–major axis, a_F, eccentricity, e_F, and argument of the periapsis, ω_F, for the final orbit, and two inequality constraints for the transfer orbit, that is, $e_T < 1$ and $r_{min} > ka_I(1 - e_I)$.

When a transfer between circular orbits is considered (Case 1), the symmetry of the problem makes θ_1 loose any influence on both the objective functions. For this reason the variable is assumed to be zero and the search space dimension is reduced to 5. All the other aspects of the optimization problem remain unchanged. A sixth constraint is added for the rendez–vous problem (Case 2), in which case the spacecraft must achieve a prescribed position at the final time, after the second impulse. This requires that also the position of the target on the final orbit is propagated.

The extension to an n–impulse case (Case 3) simply requires that more optimization variables are added and the orbit propagation algorithm is applied n times. For the three impulse case (Case 3) it is

$$\boldsymbol{x} = (\theta_1, \Delta v_1, \phi_1, \Delta\theta_1, \Delta v_2, \phi_2, \Delta\theta_2, \Delta v_3, \phi_3)^T \in \mathbb{R}^9$$

with $\theta_{i+1} = \theta_i + \Delta\theta_i$.
Inequality constraints apply to both arcs, so that a total o 4 inequality constraints need to be enforced, plus the usual three equality ones on the final orbit.

The simultaneous two–impulse transfer of two spacecraft duplicates the number of optimization variable, with respect to Case 2, with the only exception of the starting point, which is common to both satellites. The vector of optimization variables is

$$\begin{aligned} \boldsymbol{x} \quad = \quad & (\theta_1, \Delta v_{1,A}, \phi_{1,A}, \Delta v_{1,B}, \phi_{1,B}, \\ & \Delta\theta_A, \Delta\theta_B, \Delta v_{2,A}, \phi_{2,A}, \Delta v_{2,B}, \phi_{2,B},)^T \in \mathbb{R}^{11} \end{aligned}$$

and 6 equality constraints plus 4 inequality constraints are enforced.

In all the above mentioned cases, each one of the equality constraints on orbit parameters and spacecraft final anomaly (rendez–vous condition) is enforced by means of two inequality constraints in the form

$$\begin{aligned} a_{F,des} - \varepsilon_a \le a_F \le a_{F,des} + \varepsilon_a \\ e_{F,des} - \varepsilon_e \le e_F \le e_{F,des} + \varepsilon_e \\ \omega_{F,des} - \varepsilon_\omega \le \omega_F \le \omega_{F,des} + \varepsilon_\omega \\ \theta_{F,des} - \varepsilon_\theta \le \theta_F \le \theta_{F,des} + \varepsilon_\theta \end{aligned}$$

where ε_a, ε_e, ε_ω, and ε_θ are the assumed tolerances.

3.3.2 Lambert Problem

The solution of the two–point boundary value problem for Keplerian motion, also known as Lambert's problem [17], is represented by the determination of the orbit parameters of an orbit having a specified transfer time t_{des} between two prescribed positions in space, P_1 and P_2. Several algorithms have been derived for solving it, from the seminal works of prof. R.H. Battin [22] to a recent algorithm developed by G. Avanzini (see [3] and references therein).

Most of the methods are based on a parameterization of the set of orbits passing trough P_1 and P_2 with respect to some auxiliary variable. The method described in [3] exploits a novel parametrization in terms of the transverse eccentricity vector component e_t, perpendicular to the direction of the chord connecting P_1 and P_2. As far as the transfer time t_T is a monotonic function of e_t, the latter is used as the unknown for the equation $t_T(e_t) = t_{des}$.

It should be noted that, when a Lambert algorithm is used for defining the geometrical properties of either a two–impulse transfer orbit or the last trajectory arc for the n–impulse case, the constraints on the final position of the spacecraft at the end of the transfer are inherently satisfied, and the required $\Delta\vec{\boldsymbol{v}}$'s are identified by simple vector operations as

$$\begin{aligned} \Delta\vec{\boldsymbol{v}}_1 &= \vec{\boldsymbol{v}}_1 - \vec{\boldsymbol{v}}_I \\ \Delta\vec{\boldsymbol{v}}_2 &= \vec{\boldsymbol{v}}_F - \vec{\boldsymbol{v}}_2 \end{aligned}$$

where the initial and final velocities $\vec{\boldsymbol{v}}_I$ and $\vec{\boldsymbol{v}}_F$ are known from the properties of the (given) initial and final orbits, while $\vec{\boldsymbol{v}}_1$ and $\vec{\boldsymbol{v}}_2$ are determined from the orbital elements of the transfer arc.

This fact greatly simplifies the structure of the feasible solution space, inasmuch as, together with the number of equality constraints, also the number of optimization variables is reduced. This is done at the expenses of a higher computational cost for the evaluation of a single individual of the population of candidate solutions, which requires the iterative solution of the Lambert problem for the considered set of transfer parameters (starting and arrival positions on the initial and final orbits and transfer time).

For Case 1 the problem is almost over–simplified, the number of optimization variables being reduced to only two, that is,

$$\boldsymbol{x} = (\Delta\theta, t_T)^T \in \mathbb{R}^2$$

with $\theta_F = \Delta\theta$. Also Case 2 can be easily cast in a form where only two optimization variables are present,

$$\boldsymbol{x} = (t_W, t_T)^T \in \mathbb{R}^2$$

If on one side, the transfer between elliptical orbits depends on the waiting time on the starting orbit, the additional rendez–vous constraint dictates the final position at the end of the transfer, where the target position at the final time $t_W + t_T$ is easily found from the knowledge of its initial position at time $t = 0$ by application of an orbit propagation algorithm. As a matter of fact, in both these first two cases, the Pareto front could be directly traced with very simple numerical techniques.

For the three–impulse transfer (Case 3) the search space is spanned by the vector

$$\boldsymbol{x} = (t_W, t_{T_1}, r_1, \Delta\theta_1, t_{T_2})^T \in \mathbb{R}^5$$

where r_1 and $\Delta\theta_1$ assign the position of the intermediate impulse, while t_{T_1} and t_{T_2} are the transfer times along the first and the second coast arc, respectively.

On the converse, the vector of optimization variables for the simultaneous transfer of two spacecraft (Case 4) is

$$\boldsymbol{x} = (t_W, t_{T_A}, t_{T_B})^T \in \mathbb{R}^3.$$

For all the above mentioned cases, inequality constraints on eccentricity and minimum radius apply to transfer orbit segments as before, but all the equality constraints are now exactly satisfied by the problem representation itself. Although inequality constraints reduce the size of the admissible region in the search space, the subset of feasible solutions has the same dimension of the search space. A very different situation is encountered when orbit propagation is used for representing the transfer. As an example, Case 4 is characterized by 11 unknown and 8 constraints, resulting in a three–dimensional subset of feasible solutions in a 11–dimensional search space.

4. Test Methodology

The optimization algorithms adopted in this work belong to the wide class of stochastic algorithm. These methods are expected to converge to the global solution of the problem if the number of evaluations of the system model N_{eval} is sufficiently high. Equivalently, letting P_s be the probability to find the global solution, $P_s \to 1$ if $N_{eval} \to \infty$. It is obviously unpractical to allow an unbounded growth of N_{eval}, both for test cases and for real problems, so that the common practice is to stop the algorithm after a prescribed maximum number of evaluations of the system model, N_{MAX}. This means that, given a problem and an algorithm to solve it, it is important to evaluate algorithm effectiveness for a finite value of N_{MAX}. Because of the stochastic nature of the algorithms, their performance must be considered as an aleatory variable as well, whichever the metrics adopted to measure it.

4.1 Comparison metrics

All the benchmark problems considered in this work are constrained and multi-objective. Therefore the performance of the algorithms must be measured in terms of constraint satisfaction and approximation of the global Pareto front.

A first index gives information about the capability of the algorithm of finding at least one feasible solution. Given the total number of runs for the algorithm, N_{run}, the index P_{FS} is the ratio between the number of times the algorithm is able to find at least one feasible solution, N_{runF}, and the total number of runs: $P_{FS} = N_{runF}/N_{run}$.

As for the two main goals of MOEAs, that is, (i) convergence to the true Pareto optimal front, and (ii) distribution of the population over the whole front, it is necessary to introduce two parameters that evaluate both these properties. In this work, the metrics proposed by M. Vasile were adopted [23]:

$$M_{conv} = \frac{1}{N_p} \sum_{i=1}^{N_p} \min_{j \in M_p} 100 \left\| \frac{g_j - f_i}{g_j} \right\| \quad (1)$$

$$M_{spr} = \frac{1}{M_p} \sum_{j=1}^{M_p} \min_{i \in N_p} 100 \left\| \frac{f_i - g_j}{g_j} \right\| \quad (2)$$

Given the M_p solutions g_j used to describe (or to approximate) the global Pareto front, and the N_p elements f_i in the Pareto front obtained from a given run of the optimization algorithm, M_{conv} is the sum over N_p of the distance of each element in the particular front considered from the closest element of the global front. This figure of merit clearly indicates how close the obtained front is to the global one. On the other hand, M_{spr} is the sum over all the elements in the global Pareto front of the distance of each element in the global front from the closest one in the front obtained for the considered run. This parameter measures how well the individuals of the obtained front cover the whole global front.

M_{conv} and M_{spr} can assume different values for each run. A Gaussian PDF is usually assumed for these parameters, described by mean value and variance, computed by taking into account only those runs that have at least one individual in the feasible region.

4.2 Integral approach for comparison metrics

The aggregated form briefly described above reflects the common practice for the evaluation of performance indexes of stochastic algorithms, but it has a significant methodological and practical fault that needs to be underlined, because the *a priori* hypothesis that the PDFs are Gaussian is usually far from true. The actual PDF depends on a) the considered problem, b) the algorithm and c) the value of N_{MAX}. Its shape is unknown and it can be multi–modal. As an example, both multi–objective performance indexes, M_{conv} and M_{spr}, would be 0 at convergence, for $N_{MAX} \to \infty$, with a PDF represented by a Dirac function centered in zero. For $N_{MAX} < \infty$ both metrics are strictly positive by definition, so that, for very high values of N_{MAX} one expects a PDF more similar to an exponential than a Gaussian one. Only for relatively low values of N_{MAX} the values of M_{conv} and M_{spr} will be distributed on both sides of the most likely one.

For this reason, in the absence of any actual knowledge about the true shape of the PDF, a practical and useful, yet correct and rigorous approach is based on extracting from the test results the success probability, which is the probability that the considered index is beyond a predefined threshold. As an example, $P_S(M_{conv} < \theta_{conv})$ is the probability that the index M_{conv} achieves a value less than the threshold θ_{conv}. These probabilities can be evaluated over a limited number of runs with a better confidence then the PDF could be, so that it provides a more reliable merit function for optimization algorithm capabilities.

At this point, two indexes of success, $P_{FS,M_{conv}}$ and $P_{FS,M_{spr}}$, can be derived by combining constraint satisfaction probability and multi–objective requirements, that is:

$$P_{FS,M_{conv}} = P_{FS} P_S(M_{conv} < \theta_{conv}) \quad (3)$$

$$P_{FS,M_{spr}} = P_{FS} P_S(M_{spr} < \theta_{spr}) \quad (4)$$

The first one is the product of the probability to find at least one solution in the feasible region times the probability that the index M_{conv} has a value less than the threshold θ_{conv}. If one assumes that $M_{conv} = \infty$ for those runs which are not able to find feasible solutions, $P_{FS,M_{conv}}$ is equivalent to $P_S(M_{conv} < \theta_{conv})$ computed on the basis of the whole set of runs.

4.3 Critical aspects and practical solutions

In order to compute the two multi-objective metrics, M_{conv} and M_{spr}, the knowledge of the global front is required, either in analytic form or as a large set of global solutions. At the moment, such an information is not available, but it is possible to extract the best approximation of the global front from the whole set of available solutions, to be used as the reference global front.

Another important aspect that needs to be pointed out is that the statistical properties of the success indexes, defined in the form described above, can be represented by means of a binomial PDF independently of the number of function evaluations, the problem formulation and the optimization algorithm. As a major consequence of this property, brilliantly underlined by Vasile and his co–workers, [15], the test can be designed

knowing *a priori* the relation between the number of runs, N_{run}, and the error on the estimation of the success index.

A commonly adopted starting point for sizing the sample of a binomial distribution is to assume that both the normal approximation for the sample proportion p of successes (i.e. $p \sim N\{\theta_p, \theta_p(1-\theta_p)/n\}$, where θ_p is the unknown true proportion of successes) and the requirement that $Pr[|p-\theta_p| \leq d_{err}|\theta_p]$ are at least equal to $1-\alpha_p$ [24]. This leads to expression:

$$N_{run} \geq \theta_p(1-\theta_p)\chi^2_{(1),\alpha_p}/d^2_{err} \quad (5)$$

that can be approximated conservatively with

$$N_{run} \geq 0.25\chi^2_{(1),\alpha_p}/d^2_{err} \quad (6)$$

valid for $\theta_p = 0.5$.

In the framework of this preliminary test campaign, relatively modest computational resources were available, so that the above relations could not be used to size N_{run} on the basis of an acceptable error level. Rather, the same relations were used in order to estimate the error on the evaluation of the considered probability for $N_{run} = 20$. From Eq. 6 one has:

$$d_{err} \geq \sqrt{0.25\chi^2_{(1),\alpha_p}/N_{run}} \quad (7)$$

For $N_{run} = 20$, with a 95% confidence level ($\alpha_p = 0.05$), the measured success index can be affected by an error as high as $d_{err} \gtrsim 0.15$.

5. Results

In order to allow for a fair and easy comparison between the two optimization codes over the considered cases, code parameters were kept fixed, whenever possible. For the NSGA-II code, the following values were adopted: crossover probability, $p_c = 0.9$; mutation probability, $p_m = 1/dim$ (where dim is the dimension of the search space); distribution indexes for crossover and mutation, $\eta_c = 5$ and $\eta_m = 5$, respectively (values that should allow a good exploration of the search space).

For the MOPED code the parameters were: number of constraint classes, $N_{cl} = 10\% N_{ind}$; fitness coefficient, $\alpha = 0.5$; sampling proportion, $\tau = 1$.

For both codes, N_{ind} and the maximum number of generations were set for each case on the basis of the expected degree of difficulty.

All the results in terms of performance indexes are listed in Table 2. Each particular case will be detailed and commented separately in the next subsections. Only at the end, general properties and specifications will be discussed.

5.1 Transfer between circular orbits

The first and easiest test case was approached by Lambert method using $N_{ind} = 100$ and $N_{genMAX} = 20$, for a total of 2000 evaluations of the system model, with following parameters and related bounds: x_1 is the $\Delta\theta$ of the transfer arc ($x_1 \in [0.1, 2\pi - 0.1]$), x_2 is transfer time ($x_2 \in [0.05, T_F]$, where T_F is the period of the destination orbit). The minimum-fuel solution obtained by Lambert approach is shown in Figure 3.

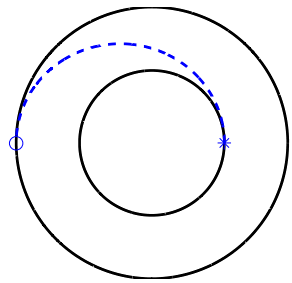

Figure 3: Min–fuel transfer manoeuvre for Case 1.

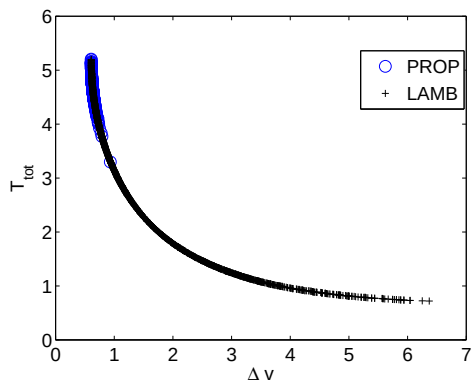

Figure 4: Best reference Pareto fronts for Case 1.

As for all the other test cases by Lambert method, both the algorithms always successfully find the feasible region, $P_{FS} = 1$, and in this particular case they apparently have the same effectiveness in covering the whole front. On the other hand, there is an appreciable difference in terms of convergence onto the best front. The whole reference front, reported in Fig. 4, is better approximated over its whole extension by the solution reported in Fig. 5, where $M_{spr} \approx 1$, then in Fig. 6, where the reported solution is characterized by $M_{spr} > 2$.

The orbit transfer is more complex to solve, when the propagation method is adopted. Due to the ad-

Table 2: Performance indexes - For all of the cases: $N_{run} = 20$, $\theta_{conv} = 0.35$, $\theta_{spr} = 1.25$

	$\bar{M}_{conv}$	$\sigma^2(M_{conv})$	$\bar{M}_{spr}$	$\sigma^2(M_{spr})$	P_{FS}	$P_{S,M_{conv}}$	$P_{S,M_{spr}}$	$P_{FS,M_{conv}}$	$P_{FS,M_{spr}}$
Case 1.L									
MOPED	0.245	0.0023	1.62	0.122	1	1	0.15	1	0.15
NSGA2	0.378	0.0073	1.48	0.067	1	0.35	0.2	0.35	0.2
Case 1.P									
MOPED	0.19	0.02	6.2	2.11	0.95	0.89	0	0.85	0
NSGA2	61.41	9996.34	88.61	10595.66	0.2	0.25	0	0.05	0
Case 2.L									
MOPED	0.07	0	5.8	15.21	1	1	0	1	0
NSGA2	0.09	0	2.04	0.14	1	1	0	1	0
Case 2.P									
MOPED	0.3	0.01	0.58	0.06	1	0.8	1	0.8	1
NSGA2	110.5	11316.4	493.56	117304.3	0.55	0	0	0	0
Case 3.L									
MOPED	20.52	165.24	5.553	2.451	1	0	0	0	0
NSGA2	4.68	27.62	4.88	27.36	1	0.2	0.25	0.2	0.25
Case 3.P									
MOPED	42.84	5048.54	115.13	20814.72	0.65	0.15	0	0.1	0
NSGA2	18.35	465.67	61.92	2632.77	0.65	0.31	0	0.2	0
Case 4.L									
MOPED	0.359	0.0026	1.19	0.00943	1	0.45	0.75	0.45	0.75
NSGA2	0.443	0.0035	1.21	0.046	1	0.05	0.65	0.05	0.65
Case 4.P									
MOPED	5.68	62.27	34.61	735.7	0.8	0.5	0	0.4	0
NSGA2	NaN	NaN	NaN	NaN	0	0	0	0	0

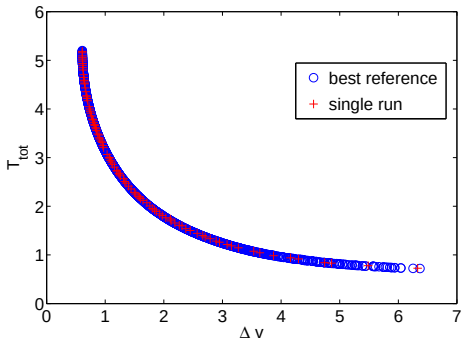

Figure 5: Run with $M_{spr} = 1.066 < \theta_{spr} = 1.25$ for Case 1. lambert

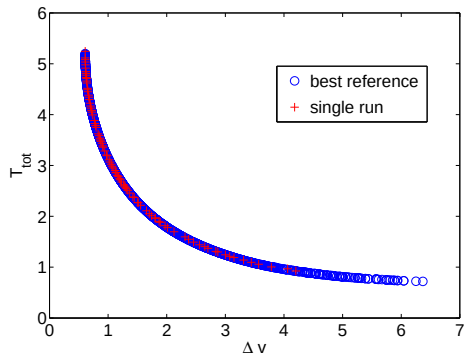

Figure 6: Run with $M_{spr} = 2.128 > \theta_{spr} = 1.25$ for Case 1. lambert

ditional constraints (in this case $\varepsilon_a = 20$ km, $\varepsilon_e = 0.005$, and $\varepsilon_\omega = 0.02$ rad), it was approached with $N_{ind} = 200$ and $N_{genMAX} = 400$, for a total of 80000 evaluations of the system model. The bounds on the search variables were as follows: magnitude of the first impulse: $x_1 \in [0.02, 1]$; direction of the first impulse: $x_2 \in [-0.2\pi, 0.2\pi]$; position of the second impulse: $x_3 \in [0.2\pi, 2\pi]$; magnitude of the second impulse: $x_4 \in [0.02, 1]$; direction of the second impulse: $x_5 \in [-0.6\pi, 0.6\pi]$.

The difference between the performance of the algorithms is evident, both in terms of P_{FS} and $P_{S,M_{conv}}$. The gap is higher than the expected error d_{err} on the evaluation of the probability, as outlined at the end of the previous section (see par. 4,3), so that it is possible to affirm with good confidence that, for this problem, the adopted version of the MOPED performs definitely better than the adopted NSGA-II code. On the other hand, both methods proved to be unable to cover the entire front.

5.2 Transfer Between Elliptical Orbits with Rendez-vous

A first more demanding test for the considered algorithms is represented by the optimization of orbit transfer between elliptical orbits, when a prescribed target on the final orbit has to be reached at the end of the maneuver. In this case, when the Lambert formulation is used, the algorithms where set with $N_{ind} = 100$ and $N_{genMAX} = 20$, for a total of 2000 evaluations of the system model, with the following parameters and related bounds: waiting time ($t_W = x_1 \in [0, 10.8$; transfer time: $t_T = x_2 \in [0.03, 10.8]$.

Both the algorithms demonstrate to be able to converge to the best front, but none of them can spread the individuals over the whole front. In Figure 7 the minimum-fuel solution obtained by Lambert approach is shown.

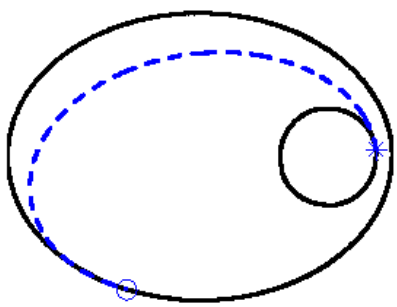

Figure 7: Min–fuel transfer manoeuvre for Case 2.

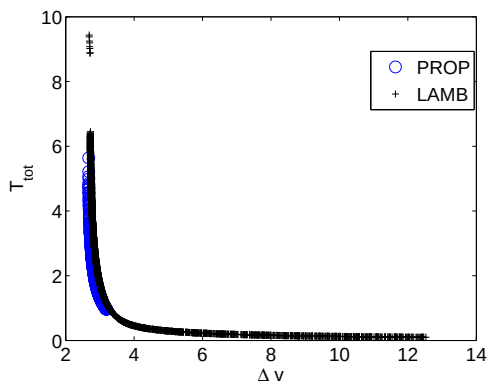

Figure 8: Best reference Pareto fronts for Case 2.

When the same case is modeled in terms of orbit propagation, the resulting optimization problem proved again to be more complex to solve. Given the additional constraints, $\varepsilon_a = 40$ km, $\varepsilon_e = 0.002$, $\varepsilon_\theta = 0.01$ rad, and $\varepsilon_\omega = 0.01$ rad, $N_{ind} = 200$ and $N_{genMAX} = 600$ were used, for a total of 120000 evaluations of the system model. The optimization parameters were bounded as follows. Position of the first impulse: $x_1 \in [-0.2\pi, 14\pi]$; magnitude of the first impulse: $x_2 \in [1.6, 4]$; direction of the first impulse: $x_3 \in [-0.2\pi, 0.2\pi]$; position of the second impulse: $x_4 \in [0.2\pi, 2\pi]$; magnitude of the second impulse: $x_5 \in [0.004, 1.6]$; direction of the second impulse: $x_6 \in [-0.6\pi, 0.6\pi]$.

Again for this constrained case the difference between the performance of the algorithms is evident, being much higher than the expected error d_{err} both in terms of P_{FS} and $P_{S,M_{conv}}$, but in the present case the MOPED algorithm successfully spreads the solutions along the front.

5.3 Three–impulse transfer

The three–impulse transfer with target on the final orbit is one of the two more complex cases handled. The version with the Lambert formulation, significantly more complex than the first two cases, was approached with $N_{ind} = 100$ and $N_{genMAX} = 300$. The optimization variables were: the waiting time, $t_W = x_1 \in [0, 1.62)$; the transfer time for the first arc, $t_{T,1} = x_2 \in [0.03, 21.54])$; the radius of the second impulse, $r_2 = x_3 \in [7010, 105410])$; the amplitude of the first transfer arc ($\Delta\theta = x_4 \in [0.01, 2\pi - 0.01]$); and the transfer time for the second arc ($t_{T,2} = x_5 \in [0.03, 21.54]$).

Even if NSGA-II shows in this case higher performance indexes, that is, it is expected to exhibit better performance than the MOPED, the difference between the two algorithms is always less than 0.30, so that, according to the reliability of the statistical estimate over a small number of run, no rigorous comparison can be derived from this test case for NSGA-II and MOPED.

In Figure 9 the minimum-fuel solution obtained by Lambert approach is shown. It should be noted that the considered algorithms demonstrated the capability of autonomously recognizing those situations where a two impulse transfer is more convenient than a three–impulse one. For the considered transfer between circular orbits, it is $r_F/r_I < 15.68$, so that a two–impulse Hohmann transfer represents the minimum–Δv solution. As a matter of fact, the minimum–Δv portion of the Pareto front is made up by solutions where one of the impulses (usually either the first or the third one) is vanishingly small, such that the initial or the final correction is practically negligible and the required transfer is achieved by two–impulses only. On the converse, for $r_F/r_I > 15.68$ (not reported for the sake of conciseness), a three–impulse bielliptical transfer was correctly identified as the optimal minimum–Δv solution.

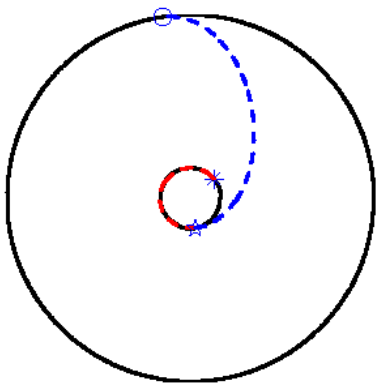

Figure 9: Min–fuel transfer manoeuvre for Case 3.

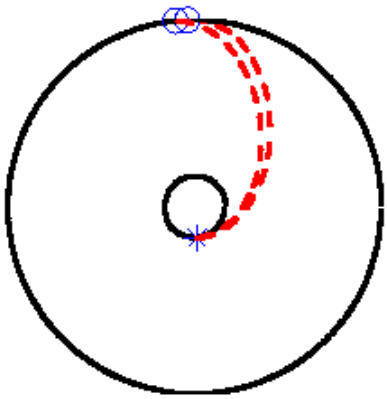

Figure 11: Min–fuel transfer manoeuvre for Case 4.

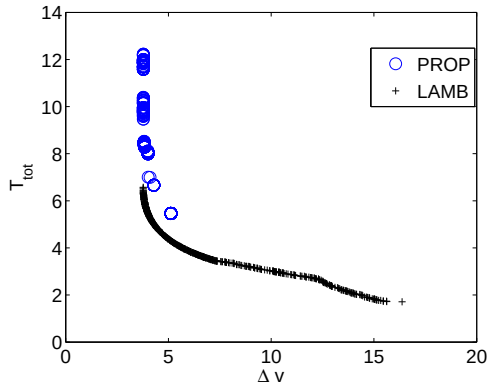

Figure 10: Best reference Pareto fronts for Case 3.

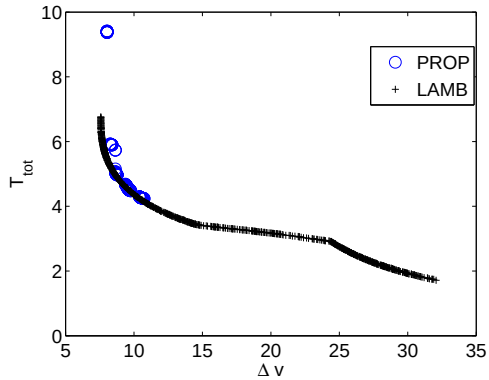

Figure 12: Best reference Pareto fronts for Case 4.

When the same case is modeled by orbit propagation, the constraints are enforced with the following tolerances: $\varepsilon_a = 140$ km, $\varepsilon_e = 0.002$, $\varepsilon_\theta = 0.01$ rad, and $\varepsilon_\omega = 0.01$ rad, while $N_{ind} = 500$ and $N_{genMAX} = 1200$, for a total of 600000 evaluations of the system model. The position of the first impulse was bounded as $x_1 \in [-2\pi/100, 2\pi]$); the magnitude of the first impulse was $x_2 \in [0.6, 3]$, while its direction was $x_3 \in [0, 0.2\pi]$; the second impulse, delivered in a position $x_4 \in [2\pi/100, 2\pi]$), had magnitude $x_5 \in [0.003, 3]$ and direction $x_6 \in [-0.4\pi, 0.4\pi]$; the third impulse was delivered in position $x_7 \in [2\pi/100, 2\pi]$, with a magnitude equal to $x_8 \in [0.003, 3]$ and a direction $x_9 \in [-0.6\pi, 0.6\pi]$).

In this case the indices demonstrate comparable performance, although a mild prevalence of NSGA-II algorithm must be recognized. It should also be noted that none of the algorithms covers the whole reference front, for the considered sets of algorithm parameters.

5.4 Simultaneous transfer of 2 satellites

Case 4 with Lambert formulation was approached with $N_{ind} = 100$ and $N_{genMAX} = 100$ and with the following parameters: waiting time $t_W = x_1 \in [0, 1.62$; transfer time for the first satellite $t_{T,A} = x_2 \in [0.03, 21.54]$; and transfer time for the second satellite ($t_{T,B} = x_3 \in [0.03, 21.54]$).

The algorithms appear equivalent in terms of both P_{FS} and $P_{S,M_{spr}}$, but MOPED looks superior in terms of $P_{S,M_{conv}}$. In Figure 9 the minimum-fuel solution obtained by the Lambert approach is shown.

When the case is modeled by a propagation method, $N_{ind} = 400$ and $N_{genMAX} = 800$ (for a total of 320000 evaluations of the system model) and the same constraints of Case 3 were enforced. The optimization variables were bounded as follows. The position of the first impulse for both satellites A and B is $x_1 \in [-2\pi/100, 2\pi]$); the magnitude of the first impulse for satellite A is $x_2 \in [1.5, 3]$; its direction $x_3 \in [0, 0.2\pi]$);

the position of the second impulse for satellite A is $x_4 \in [2\pi/100, 2\pi]$; its magnitude $x_5 \in [0.003, 2.7]$), while its direction is $x_6 \in [-0.6\pi, 0.6\pi]$; the magnitude of the first impulse for satellite B is $x_7 \in [1.5, 3]$, with direction $x_8 \in [0, 0.2\pi]$; the position of the second impulse for satellite B is $x_9 \in [2\pi/100, 2\pi]$, with a magnitude equal to $x_{10} \in [0.003, 2.7]$ and a direction $x_{11} \in [-0.6\pi, 0.6\pi]$.

In this case a comparison is not possible because none of the 20 runs of the NSGA-II provided any feasible solution. The result is somehow unexpected and will be investigated.

5.5 Remarks and comments

There are few comments and remarks that need to be pointed out. First of all, it appears evident from the tests that an approach by propagation method is not the best choice. Compared to the the Lambert approach, propagation requires to handle a higher number of design variables and constraints and, even if the MOPED algorithm appears capable of always reaching the feasible region, the optimization approach becomes extremely expensive.

Also, discrepancies between the best reference fronts obtained by the two modeling approaches demonstrate two major findings of this research: a) constraints, especially for more complex cases, tend to bias the search towards a relatively limited portion of the feasible region of the search space; this means that the coverage of the entire front in one run becomes unlikely and, since our reference fronts are the union of relatively few runs, they are not even complete; b) ideally, in order to find a truly global solution of the problem, the search for all the design variables should be allowed to vary between $-\infty$ and ∞; this was not done, in order to avoid regions where the model is not valid and to limit the computational time, but in such a way it is not easy to provide the considered approaches with exactly equivalent search spaces.

A second observation concerns the unquestionable superiority of the Lambert approach. Even if it can be considered as demonstrated, the presented results can only be seen as "qualitative" and "relative", because of the relatively small number of test runs for each case. The aim of this work was to provide new ideas for future extensive tests, that, based on a wider range of results, will allow for a more correct interpretation of the data. At present the obtained index values are affected by the following problems:

- a low value of N_{run}, in this case, influences twice the precision of the results: a) a high value of d_{err} allows to distinguish between the algorithms only when the discrepancy in terms of indexes is very high; b) the best Pareto front is itself a product of the runs, therefore also the confidence on the reference front is low when N_{run} is small;
- since θ_{conv} and θ_{spr} are fundamental for the determination of the merit index, a standard value for all of the cases may not be the best choice.

Part of the future work will be aimed at standardizing the models, both in terms of variable bounds and constraint levels ($\epsilon_a, \epsilon_e, \epsilon_\theta$ and ϵ_ω), in order to use them as benchmarks for constrained optimization algorithms.

6. Conclusions and Future Work

An approach for comparing performance of Evolutionary Optimization Algorithms has been developed and tested over a set of 4 benchmark case, using two different multi–objective optimization codes: a standard genetic algorithm and a Parzen–based estimation of distribution algorithm. Two different representation of the orbit transfer problem were also adopted, for a total of 4 possible different optimization approaches. With respect to the second aspect, modeling the transfer orbit by solving a Lambert problem allows for a direct enforcement of constraints on the final position (including rendez–vous), which greatly simplifies the solution of the optimization problems, by reducing the number of optimization variables at stake. At the same time, orbit propagation still offers a good benchmark for testing the capabilities of different algorithms over constrained problems. As for the optimization codes, the adopted version of MOPED algorithm performs usually better than the adopted version of NSGA-II, although the limited number of runs available makes this statement somehow questionable and the comparison only qualitative.

In this respect, considering the proposed comparison metrics for multi–objective optimization as representative of the actual performance of the algorithms, future research will be addressed towards improving (i) the evaluation of the statistical properties of the performance indices adopted, by means of a higher number of runs, and (ii) the standardization of the test cases, by making the search space truly equivalent.

References

1. K. Deb, *Multi-Objective Optimization Using Evolutionary Algorithms*. John Wiley & Sons, NY, 2002.

2. M. Costa, E. Minisci, "MOPED: a Multi-Objective Parzen-based Estimation of Distribution algorithm", Second International Conference on Evolutionary Multi-Criterion Optimization, EMO 2003, Faro, Portugal. Springer - LNCS 2632. 2003, pp. 282–294

3. G. Avanzini, "A Simple Lambert Algorithm", *J. Guid. Control & Dyn.*, Vol. X(5), 2008, in print.

4. L. Casalino, G. Colasurdo, and D. Pastrone, "Indirect approach for minimum-fuel aeroassisted transfers," AIAA/AAS Astrodynamics Conference, San Diego, CA, July 1996, AIAA Paper 96–3592.

5. M. La Mantia, and L. Casalino, "Indirect Optimization of Low-Thrust Capture Trajectories," *J. Guid. Control & Dyn.*, 29(4), 2006, 1011–1014.

6. C.L. Ranieri, and Cesar A. Ocampo, "Indirect Optimization of Two-Dimensional Finite Burning Interplanetary Transfers Including Spiral Dynamics," *J. Guid. Control & Dyn.*, 31(3), 2008, 720–728.

7. D.P. Bertsekas, *Constrained Optimization and Lagrange Multiplier Methods*, Athena Scientific, 1996.

8. T. Bäck, *Evolutionary Algorithms in Theory and Practice: Evolution Strategies, Evolutionary Programming, Genetic Algorithms*, Oxford Univ. Press. 1996.

9. M. Mitchell. *An introduction to genetic algorithms*, MIT Press, 1998.

10. H.G. Beyer, and H.P. Schwefel, "Evolution Strategies: A Comprehensive Introduction", Journal Natural Computing, 1(1):3-52, 2002.

11. K.V. Price, R.M. Storn, and J.A. Lampinen. *Differential Evolution. A Practical Approach to Global Optimization.* Natural Computing Series, Springer, 2005.

12. G. Avanzini, E.A. Minisci, and D. Biamonti, "Minimum-Fuel/Minimum-Time Maneuvers of Formation Flying Satellites", AAS/AIAA Astrodynamics Specialist Conference, Big Sky, Montana (USA), August 2003. AAS Paper 03-654.

13. C.R. Bessette, and D.B. Spencer, "Performance Comparison of Stochastic Search Algorithms on the Interplanetary Gravity-Assist Trajectory Problem," *J. Spacecraft & Rockets*, 44(3), 2007, 722-724.

14. P.L. Di Lizia, G.M. Radice, D. Izzo, M. Vasile, "On the Solution of Interplanetary Trajectory Design Problems by Global Optimisation Methods", Proceedings of GO 2005, pp. 1–7.

15. M. Vasile, E. Minisci, and M. Locatelli, "On Testing Global Optimization Algorithms for Space Trajectory Design", AIAA/AAS Astrodynamics Specialist Conference and Exhibit, Honolulu, Hawaii (USA), August 2008, AIAA paper 2008-6277.

16. K. Deb, A. Pratap, S. Agarwal, and T. Meyarivan, "A Fast and Elitist Multiobjective Genetic Algorithm: NSGA-II", IEEE Transactions on Evolutionary Computation, 6(2), April 2002.

17. R.H. Battin, *An Introduction to the Mathematics and Methods of Astrodynamics*, Revised Ed. , AIAA Education Series, Reston, Virginia (USA), 1999, Chpts. 4, 5.

18. A.K. Reichert, "Using a Genetic Algorithm to Determine the Optimum Two-Impulse Transfer Between Co-Planar, Elliptical Orbits," in *Industrial Applications of Genetic Algorithms*, C.L. Karr and L.M. Freeman editors, CRC Press, Boca Raton, FL (USA), 1999, pp. 111–133.

19. Y.H. Kim, and D.B. Spencer, "Optimal Spacecraft Rendezvous Using Genetic Algorithms," *J. Spacecraft & Rockets*, 39 (6), 2002, 859–865.

20. O. Abdelkhalik, and D. Mortari, "N-Impulse Orbit Transfer Using Genetic Algorithms," *J. Spacecraft & Rockets*, 44(2), 2007, 456–459.

21. N. Khan, D.E. Golberg, and M. Pelikan, "Multiobjective Bayesian Optimization Algorithm", Technical Report IlliGAL 2002009, University of Illinois at Urbana-Champain - IlliGAL, 2002.

22. R.H. Battin, "An Elegant Lambert Algorithm," *J. Guid. Control & Dyn.*, 7(6), 1984, 662–670.

23. M. Vasile, "Hybrid Behavioural-Based Multiobjective Space Trajectory Optimization", on *Multi-Objective Memetic Algorithms*, Springer Series of Studies in Computational Intelligence, 2008, to appear.

24. C.J. Adcock, "Sample size determination: a review". *The Statistician*, 46(2):261–283, 1997.